Received: 11 August 2022 | Revised: 10 November 2022 | Accepted: 6 December 2022

DOI: 10.1002/ese3.1373

ORIGINAL ARTICLE

# Multi-stage cold energy recovery/utilization: A 10 MW class cold store with liquefied natural gas

Jinxin Yue[1] | Juan Feng[1] | Jingyu Chen[1] | Rui Liu[1] | Chengbiao Yu[1] | Zhaomin Jiang[1] | Xiaoyuan Chen[1] | Boyang Shen[2,3] | Lin Fu[2,4]

[1]School of Engineering, Sichuan Normal University, Chengdu, China

[2]Department of Engineering, University of Cambridge, Cambridge, UK

[3]Clare Hall, University of Cambridge, Cambridge, UK

[4]VLSI Research Europe, Cambridge, UK

**Correspondence**

Juan Feng and Xiaoyuan Chen, School of Engineering, Sichuan Normal University, Chengdu 610101, China.
Email: fengjuan@sicnu.edu.cn and chenxy44@sina.com

Boyang Shen and Lin Fu, Department of Engineering, University of Cambridge, Cambridge CB3 0FA, UK.
Email: bs506@cam.ac.uk and lin.fu.2017@outlook.com

**Funding information**

Sichuan Science and Technology Program, Grant/Award Number: 2022YFG0304; National Training Program of Innovation and Entrepreneurship for Undergraduates, Grant/Award Number: 202110636002

**Abstract**

In coastal cities, a large amount of cold energy is released into the nearby seawater during the process of regasification of liquefied natural gas (LNG) at the receiving terminal, and meanwhile, a large amount of exported and/or imported foods need to be frozen by bulk cold energy near the sea. In this paper, a new multistage cold energy recovery/utilization system is investigated to link the LNG cold energy directly to supply the coastal cold store. This design uses a realistic case in Ningbo LNG receiving station in China, and for the very first time considers how to utilize the LNG cold energy in an efficient manner regarding the technical, economic, and environmental benefits. A three-stage LNG cold energy utilization system is designed and evaluated by considering different temperatures, pressures, and heat exchange parameters. Compared to conventional electric-driven cold stores, the proposed multistage cold energy recovery/utilization system has a much cheaper capital cost during the initial investment stage, and also avoids the utility power consumption during the daily operation period. In the case study, from Ningbo LNG receiving station to a 10 MW class cold store, the proposed multienergy system can save the energy of 20.05 kilotons of standard coal, and the carbon emission reduction is up to $1.49 \times 10^8$ kg per year.

**KEYWORDS**

cold energy recovery, cold store, heat exchange, liquefied natural gas, LNG regasification

## 1 | INTRODUCTION

As the global energy crisis and environmental pollution are steadily deteriorating, the question that how to efficiently recycle and re-use different energy resources has become a wide concern over the recent years. As one of the clean fuels,[1,2] liquefied natural gas (LNG) mainly depends on long-distance shipping. Figure 1 shows a typical LNG supply chain from a remote gas mining field to a local end-user side. The natural gas is exploited from deep underground and then liquefied into LNG for high-density fuel reserve.[3] In general, about 625 $m^3$ of natural gas at one atmosphere of pressure can be compressed into 1 $m^3$ LNG.[4,5] After then, the LNG fuel is shipped to distant coastal cities. At the LNG receiving terminals, the LNG fuel needs to be regasified and finally transported to the end-user sides.[6,7]

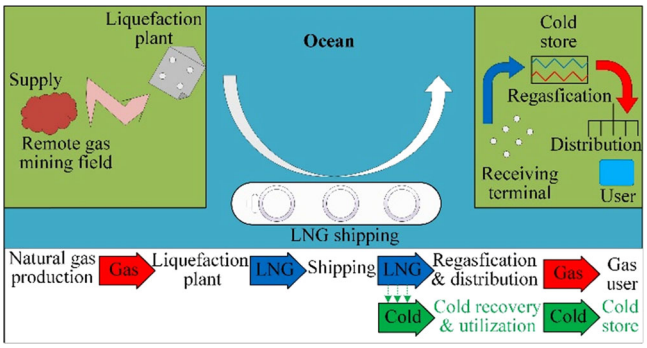


**FIGURE 1** Schematic diagram of the LNG supply chain with the multistage cold energy recovery/utilization.

As the temperature of LNG is −162°C under a normal storage conditions, plenty of cold energy can be released during the LNG gasification and the subsequent temperature increase of cold natural gas.[8] However, in many cases the LNG regasification is implemented by the cold energy exchange operations with nearby seawater. During the regasification, a large amount of cold energy is wasted. What's worse, the discarded cold energy also causes negative impacts on the marine ecoenvironment.[9]

To avoid energy waste and potential environmental risks, many scholars and institutions have put forward a number of energy recovery and utilization solutions regarding LNG regasification, such as electric power generation,[10] air separation,[11] low-temperature energy storage,[12] dry ice production,[13] seawater desalination,[14] food processing,[15] and so forth.

Since the LNG regasification operates without stopping, the released cold energy can be considered as a continuous energy source, which fits well with relatively stable energy loads. At present, although there are a series of cold energy utilization schemes, there are still several technical and economic challenges.[16] For instance, LNG cold energy is able to produce dry ice for cold energy storage, but this phase-change material is easy to block the pipes, and the overall system needs relatively high maintenance costs.[17] LNG cold energy is able to generate a certain amount of electricity for local use, but the overall energy efficiency is relatively low. Although the efficiency can be greatly improved when integrating with other energy technologies and subsystems, the corresponding capital investment cost is also greatly increased.[10,18–20]

To solve the technical difficulty and reduce capital costs simultaneously, in this article we attempt to investigate a new solution for the LNG cold energy recovery/utilization for coastal cold store applications. The motivations, novelties, and contributions are summarized as follows:

1) In terms of the actual application demand, there are a large amount of goods and foods that need to be frozen near the sea. One main part is the frozen foods which have already arrived at the local seaport, and the other part is the fresh foods which will be soon shipped out. The frozen foods shipped from abroad need to be kept at a suitable temperature for long-time food preservation, and the fresh foods should be frozen before long-distance sea transportation. Therefore, building a local cold store near the seaport is fairly necessary for the actual import and export.
2) In terms of the cold energy demand, conventional cold stores consume a great amount of coal-based utility power and then cause indirect greenhouse gas emissions. If the LNG cold energy can be kept at the working temperature inside the cold store, there will be no need to consume additional electricity for generating cold energy.
3) In terms of capital investment for refrigeration equipment, conventional cold stores need a lot of compressors and air conditioners (ACs) to convert electric energy into cold energy. By comparison, the LNG-based cold store requires very few compression equipments, and then saves a lot of costs.
4) In terms of the capital investment for energy exchangers, conventional LNG regasification needs to configure a number of single-stage heat exchangers which releases the cold energy into seawater.[21] For the new cold store, the original cost for purchasing single-stage heat exchangers can be used to buy multistage heat exchangers to meet the requirements in a more efficient way.

## 2 | SYSTEM DESIGN AND OPERATION PRINCIPLE OF MULTISTAGE LNG COLD ENERGY RECOVERY/UTILIZATION

### 2.1 | Cold store design

The Ningbo LNG receiving station includes an area of 46.9 ha and has a total capacity of 6 million tons of LNG per year.[22] Near the receiving station, there is a large amount of cold energy released during the regasification. In this article, about 5 million tons of LNG are assumed to be regasified through the multistage heat exchangers and then supply the recovered cold energy for a 10 MW class coastal cold store.

The designed cold store is mainly composed of a meat freezing room (MFR), aquatic product freezing room (APFR), storage room (SR), ice making room (IMR), and ice storage room (ISR). The overall area of the SR is about 33,000 $m^2$, and the volume utilization ratio is 65%. Inside the SR, the stacking densities of frozen meats and aquatic products are 0.4 and 0.47 $t/m^3$, respectively. The overall area

TABLE 1 Main parameters of the five functional areas in the 10 MW class cold store.

| Module | Mass (ton) | Cooling load (W/t) | Mechanical load (W/ton) | Total load (W/ton) | Inlet temperature (°C) | Outlet temperature (°C) | Input power (kW) |
|---|---|---|---|---|---|---|---|
| MFR | 1000 | 7600 | 5800 | 13,400 | 35 | −15 | 11,170 |
| APFR | 4500 | 7000 | 5600 | 12,600 | 20 | −15 | 37,800 |
| SR | 40,590 | 28 | 21 | 49 | – | – | 1989 |
| IMR | 380 | – | 7000 | 7000 | 20 | −10 | 2660 |
| ISR | 2530 | – | 25 | 25 | – | – | 63.25 |

Abbreviations: APFR, aquatic product freezing room; IMR, ice making room; ISR, ice storage room; MFR, meat freezing room; storage room.

TABLE 2 Main parameters of the two refrigerants in the three-stage LNG cold energy recovery/utilization process.

| Modules | Medium | Inlet pressure (MPa) | Outlet pressure (MPa) | Inlet temperature (°C) | Outlet temperature (°C) |
|---|---|---|---|---|---|
| MFR | Liquid ammonia | 0.15 | 0.149 | −25 | −55 |
| APFR | Liquid ammonia | 0.15 | 0.149 | −25 | −55 |
| SR | Liquid ammonia | 0.15 | 0.149 | −20 | −55 |
| IMR | Liquid carbon dioxide | 3 | 2.97 | −20 | 0 |
| ISR | Liquid carbon dioxide | 3 | 2.97 | −20 | 0 |
| AC | Liquid carbon dioxide | 3 | 2.97 | −10 | 10 |

Abbreviations: AC, air conditioner; APFR, aquatic product freezing room; IMR, ice making room; ISR, ice storage room; LNG, liquefied natural gas; MFR, meat freezing room; storage room.

of the ISR is about 1500 $m^2$, and the volume utilization ratio is 49%. The freezing efficiency of the freezing room is 2.4 $m^2$/d/t, and the freezing area of the 5500 tons of goods stored is about 13,200 $m^2$. The main parameters of the five functional areas in the 10 MW class cold store are shown in Table 1. In addition to supplying the cold store, the three-stage LNG cold energy recovery/utilization system can also provide an abundance of cold energy in the ACs, which are normally used in nearby buildings and residents.

In normal operation, the cold storehouse purchases 1000 tons of fresh meat and 4500 tons of fresh aquatic products every day. These fresh foods need to be firstly frozen and then kept in constant cold storage. In addition, the local city imports about 118,000 tons of frozen meat and 97,000 tons of frozen aquatic products every year.[23] During the subsequent transportation process of aquatic products, about 5%–10% of the ice needs to be added for ensuring the quality of aquatic products. If a median value of 7.5% is adopted, about 380 tons of ice needs to be made every day.

## 2.2 | Energy exchange modeling

The multistage heat exchanger in the 10 MW class cold store has three different energy exchange stages. Thanks to the advantages of low material cost and high latent heat, liquid ammonia was used as the refrigerant in the first stage (Stage I) and the second stage (Stage II). Under the pressure of 0.15 MPa, its freezing point and boiling point are −77.7°C and 25.2°C, respectively. In the third stage, liquid carbon dioxide is used as the refrigerant, and its freezing point and boiling point are −56°C and −5.55°C, under the pressure of 3 MPa.

Table 2 summarizes the main parameters of the two refrigerants in the three-stage LNG cold energy recovery/utilization process. Due to the phase transition of liquid ammonia, the energy in the heat transfer process includes three parts: (1) the energy absorbed or released by the temperature change of liquid ammonia, (2) the energy absorbed or released by the temperature change of gaseous ammonia, and (3) the latent heat of gasification of liquid ammonia into gaseous ammonia. The temperature range of ammonia in the first stage and the second stage is between −55°C and −25°C. In the third stage, the temperature range of carbon dioxide in the ice-making module and the ice-storage module is between −20°C and 0°C, and the temperature range of the air conditioning system is between −10°C and 10°C. These two refrigerants in the heat transfer process will not solidify and block the pipeline, and there is also a process of gasification and liquefaction that will greatly improve the cooling capacity.

In order to evaluate the use of LNG for establishing the cold store, we made the following assumptions[20,24]:

- The system is in a steady state.
- The energy loss of the liquid in the pipeline is ignored.
- The circulating pump is based on an isentropic efficiency model.
- The temperature change caused by the boosting process of the pump is ignored.
- Heat transfer complies with energy conservation and pinch limits.

In the gasification process of LNG, the cold energy released is:

$$W_{\mathrm{LNG}} = m_{\mathrm{LNG}} \times (h_{\mathrm{L-3}} - h_{\mathrm{L-2,S}} + h_{\mathrm{L-4}} - h_{\mathrm{L-3,S}} + h_{\mathrm{L-8}} - h_{\mathrm{L-5,S}} + h_{\mathrm{L-9}} - h_{\mathrm{L-6,S}} + h_{\mathrm{L-10}} - h_{\mathrm{L-7,S}}), \quad (1)$$

where $m_{\mathrm{LNG}}$ is the mass flow rate of LNG, $h$ stands for enthalpy, and the subscript "s" stands for the isentropic process.

The cold energy obtained by the refrigerant of each module from the LNG can be calculated by:

$$W_{\mathrm{RE,r}} = \eta \times (m_{\mathrm{LNG}} \times (h_{\mathrm{L-3}} - h_{\mathrm{L-2,S}} + h_{\mathrm{L-4}} - h_{\mathrm{L-3,S}}) + m_{\mathrm{L-5}} \times (h_{\mathrm{L-8}} - h_{\mathrm{L-5,S}}) + m_{\mathrm{L-6}} \times (h_{\mathrm{L-9}} - h_{\mathrm{L-6,S}})), \quad (2)$$

where $\eta$ is the heat transfer efficiency of the heat exchanger.

The cold energy obtained by the refrigerant in the air conditioning system from the LNG can be calculated by:

$$W_{\mathrm{AC,r}} = m_{L-7} \times (h_{L-10} - h_{L-7,\mathrm{S}}). \quad (3)$$

The cold energy obtained by each module of the cold store can be calculated by:

$$W_{\mathrm{RE}} = \eta_{\mathrm{e}} \times \sum_{\mathrm{i}=1}^{8} (m_{\mathrm{E-i}}(h_{\mathrm{i,out}} - h_{\mathrm{i,in}})), \quad (4)$$

where $m_{\mathrm{E\text{-}i}}$ is the mass flow through the primary side refrigerant of the E-i heat exchanger, $h_{\mathrm{i,out}}$ and $h_{\mathrm{i,in}}$ are the enthalpy values of the E-i inlet and outlet, respectively. $\eta_{\mathrm{e}}$ is the heat transfer efficiency of the heat exchanger.

The cold energy obtained by the air conditioning system can be calculated by:

$$W_{\mathrm{AC}} = m_{\mathrm{E-9}}(h_{\mathrm{R-27}} - h_{\mathrm{R-26,S}}). \quad (5)$$

The cold energy utilization efficiency of LNG is:

$$\eta_{\mathrm{cold}} = \frac{W_{\mathrm{RE}} + W_{\mathrm{AC}}}{W_{\mathrm{LNG}}}. \quad (6)$$

During the system operation, the energy consumption to maintain the system pressure is

$$W_{\mathrm{P}} = \frac{\sum_{\mathrm{i}=1}^{6} (m_{\mathrm{P-i}} \times (h_{\mathrm{i,out}} - h_{\mathrm{i,in}}))}{\eta_{\mathrm{P}}}, \quad (7)$$

where $m_{\mathrm{P\text{-}i}}$ is the mass flow through the P-i booster pump, $h_{\mathrm{i,out}}$ and $h_{\mathrm{i,in}}$ are the P-i import and export enthalpy values, respectively.

## 3 | OVERALL SYSTEM MODELING AND ENERGY EXCHANGE PROCESS

Figure 2 shows the overall system diagram of the three-stage LNG cold energy recovery/utilization system. The main energy exchange process is described as follows.

(1) First-stage cold energy utilization: The LNG is firstly pressurized to 7 MPa by a P-1 compressor, and then carried out the cold recovery between a heat exchanger LNG-1 and liquid ammonia. In this process, the LNG at 162°C is heated up to low-temperature NG at −105.5°C, while the liquid ammonia is cooled down from −25°C to −55°C. After that, the liquid ammonia is pressurized by a P-2 compressor to maintain the pressure inside the liquid ammonia pipeline. After being separated by the S-1 liquid diverter, the liquid ammonia is finally transported to three heat exchangers (E-1, E-2, E-3) for freezing the foods inside the cold store.
(2) Second-stage cold energy utilization: When the LNG flows through the LNG-1, the generated low-temperature NG at −105.5°C then enters the LNG-2 for the second-stage heat exchange with liquid ammonia. In this process, the low-temperature NG is further heated up to −60°C, and the liquid ammonia is also cooled down from −25°C to −55°C. Note that the total recovered energies in the first and second stages are used in the frozen meat room, the frozen aquatic product room, and the SR.
(3) Third-stage cold energy utilization: After passing through the S-5, the low-temperature NG at −60°C is used to cool the liquid carbon dioxide through three heat exchangers (LNG-3, LNG-4, LNG-5). The three channels of NG are designed to be heated up to

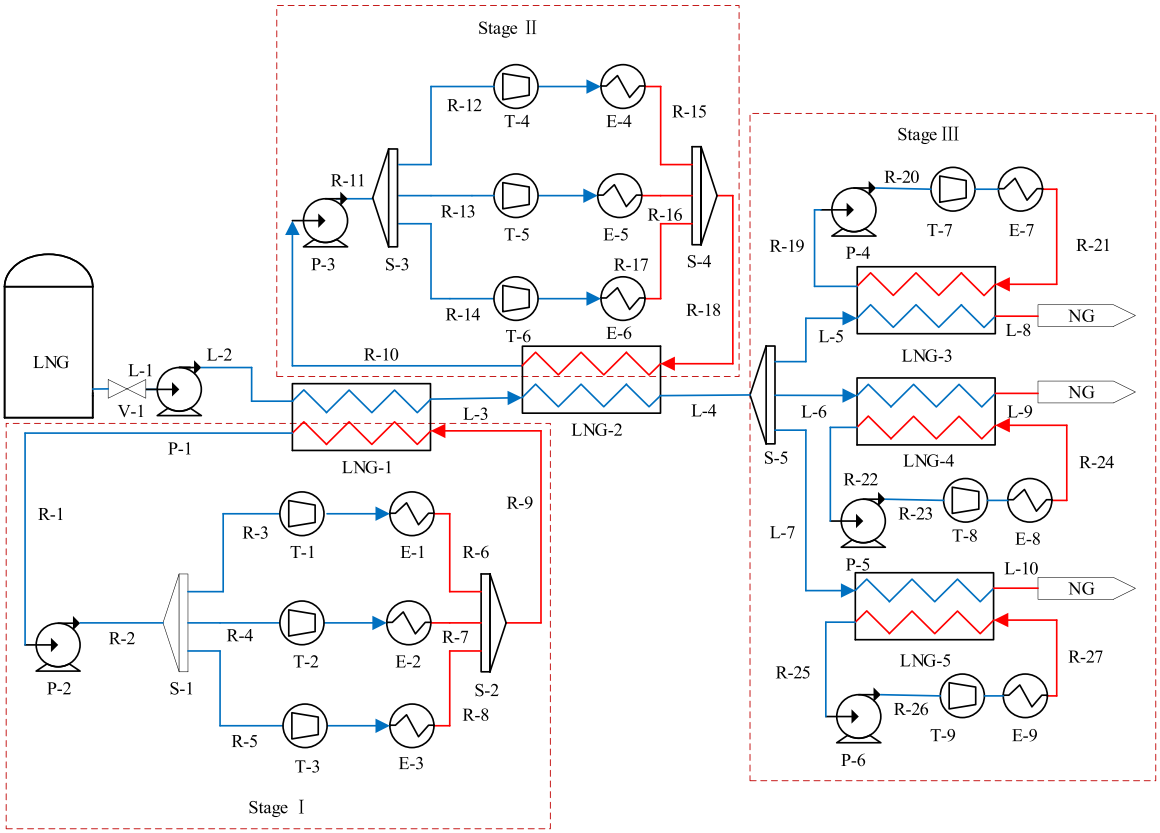


**FIGURE 2** Schematic diagram of the three-stage liquefied natural gas (LNG) cold energy recovery/utilization system for a 10 MW class cold store.

−25°C, −25°C, and −15°C, and finally sent to the NG main pipes for long-distance transportation. Accordingly, the three types of liquid carbon dioxide are cooled to −20°C, −20°C, and −10°C, respectively. Finally, the liquid carbon dioxide passes through the three heat exchangers (E-7, E-8, E-9) to provide the cold energy demanded by the ice-making, ice storage, and air conditioning systems.

It should be noted that: according to different temperatures of the cold store, the proposed system uses the high-quality cold energy with lower temperature (LNG from −162°C to −60°C) for the frozen and SRs, while, the relatively low-quality cold energy with higher temperature (NG from −60°C to −15°C) is used for the ice making, ice storage, and air conditioning systems. Considering the utilization efficiency of cold energy and the costs of the heat exchange equipment,[25] the LNG from −162°C to −60°C can be further divided into two divisions: Division I and Division II. For Division I, where the LNG is from −162°C to −105.5°C, a part of the refrigerant is in the gas–liquid mixed state, and thus the small and thinner pipelines for heat exchange/convection can be used to reduce costs. For Division II, where the NG is from −105°C to −60°C, the refrigerant is fully gaseous with higher pressure, and thus larger and thicker pipelines should be used for higher flowing speed and better pipe stability.

The default operating parameters of the system are listed in Table 3. The overall simulation model is based on Matlab/Simulink. Relevant operating parameters of LNG, liquid ammonia, and carbon dioxide can be found in the software REFPROP 9.11.

## 4 | MULTISTAGE SIMULATION AND ANALYSIS

### 4.1 | LNG gasification procedure

Before the process of LNG gasification, the pressure is 0.1 MPa, the temperature is −162°C, and the mass flow rate is 172.45 kg/s at the L-1 node, as shown in Figure 3. After the initial pressurization at P-1, the pressure reaches 7.21 MPa at the L-2 node. The enthalpy value is 5.94 kJ/kg. After passing through two heat exchangers (LNG-1, LNG-2), the temperatures at L-3 and L-4 nodes increase to −105.5°C and −60°C. The pressures are 7.14 and 7.07 MPa, and the enthalpies are 195.82 and 467.54 kJ/kg, respectively.

TABLE 3 Default parameters of the proposed cold store system.

| Parameters | Value |
|---|---|
| Ambient temperature | 25°C |
| LNG inlet temperature | −162°C |
| LNG inlet pressure | 7.21 MPa |
| Mass flow rate of LNG | 172.45 kg/s |
| LNG outlet temperature | −25/−15°C |
| Natural gas transportation pressure | 7 MPa |
| Pressure drop | 1%[20] |
| Isentropic efficiency of compressor | 80%[26] |
| Effectiveness of the heat exchangers | 80%[27] |
| Pressure of pressurized carbon dioxide | 3 MPa |
| Pressure of pressurized ammonia | 0.15 MPa |

Abbreviation: LNG, liquefied natural gas.

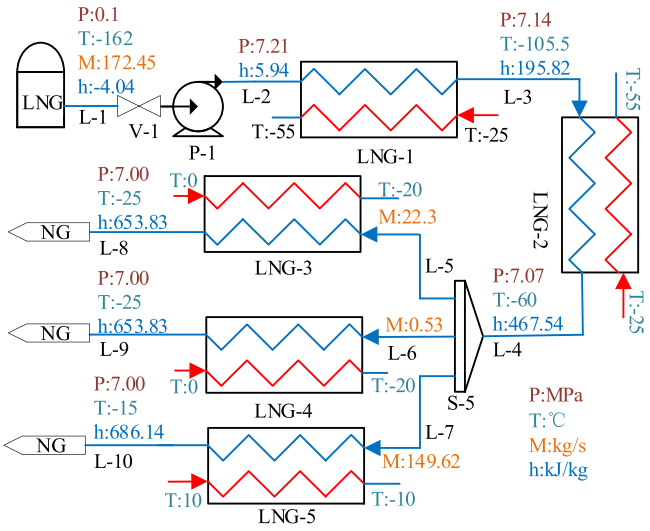


FIGURE 3 Parameter changes during the liquefied natural gas (LNG) gasification.

Through the S-5 diverter, the low-temperature NG is divided into three parts. Their mass flows are 22.3, 0.53, and 149.62 kg/s, respectively. Finally, after passing through the LNG-3, LNG-4, and LNG-5 heat exchangers, the three channels of low-temperature NGs are heated to −25°C, −25°C, and −15°C, respectively. The enthalpies are 653.83, 653.83, and 686.14 kJ/kg, and the pressure drop is 7.00 MPa.

## 4.2 | First-stage energy exchange procedure

The first cold energy utilization stage uses liquid ammonia as the refrigerant. After the cooling operation with the LNG-1 heat exchanger in Figure 4, the pressure at the R-1 node is

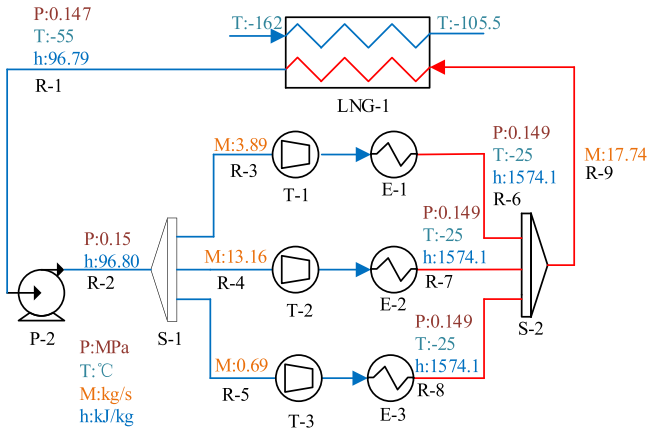


FIGURE 4 Parameter changes during the first-stage energy exchange.

0.147 MPa, the temperature is −55°C, the enthalpy is 96.79 kJ/kg, and the mass flow rate is 17.74 kg/s. After the P-2 booster pump, the pressure at the R-2 node is 0.15 MPa. The mass flow rates at the R-3–R-5 nodes are 3.89, 13.16, and 0.69 kg/s, respectively. After the continuous cooling operation with three heat exchangers E-1–E-3, the temperature of the refrigerant increases to −25°C, and the pressure decrease to 0.149 MPa again.

## 4.3 | Second-stage energy exchange procedure

The second cold energy utilization stage is similar to the first stage. The pressure and temperature of each node are the same as those of the first stage, as shown in Figure 5. The difference is that both the mass flow of refrigerant and the cold energy provided to each cold store module have been changed according to the actual cooling demands. To improve the utilization efficiency of LNG cold energy, two stages of cold energy can be used together in multiple cold store modules. The mass flow rate at the R-10 node is 252.2 kg/s. After passing through the S-3 diverter, the mass flow rates at R-12–R-14 nodes are 5.57, 18.83, and 0.99 kg/s, respectively.

## 4.4 | Third-stage energy exchange procedure

In the third cold energy utilization stage, the NG cold energy is mainly used for ice making, ice storage, and air conditioning system. In the ice-making module, the pressure, temperature, mass flow, and enthalpy of carbon dioxide at the R-19 node are 2.94 MPa, −20°C, 17.85 kg/s, and 154.28 kJ/kg, respectively. The refrigerant is pressurized to 3 MPa through a P-4 compressor and then used to

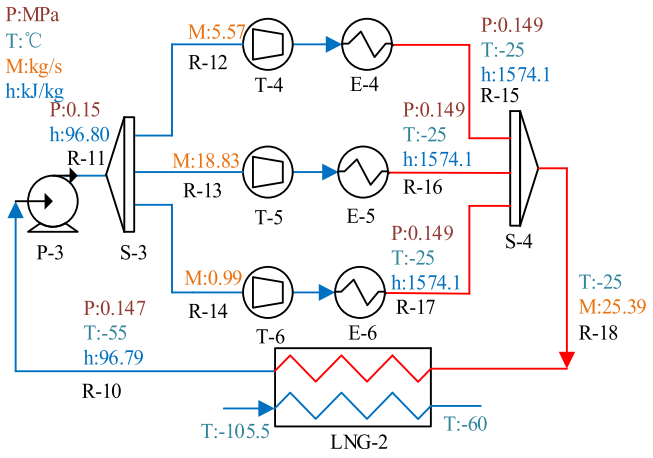


**FIGURE 5** Parameter changes during the second-stage energy exchange.

produce ice through the E-7 heat exchanger. In this ice-making process, the refrigerant pressure is reduced to 2.97 MPa and the temperature is raised to 0°C again. The enthalpy is 442.84 kJ/kg. In the ice storage module, the pressure and temperature of each node are the same as those of the nodes of the ice-making module. The difference is that the mass flow of refrigerant is 0.42 kg/s.

In the air conditioning module, after the cooling operation with the LNG-5 heat exchanger, the pressure of the refrigerant is 2.94 MPa, the temperature is −10°C, the enthalpy is 176.34 kJ/kg, and the mass flow is 119.2 kg/s at R-25 node. It is further pressurized to 3 MPa through the P-6 compressor and then provides cold energy through the heat exchanger E-9. The obtained cold energy is finally used in the air conditioning systems for the use of nearby buildings and residents. In this air conditioning process, the refrigerant pressure is reduced to 2.97 MPa and the temperature is raised to 10°C again. Under this condition, the enthalpy changes to 456.47 kJ/kg.

## 4.5 | Results and analyses

For the overall simulation model of the 10 MW class cold store built in Matlab/Simulink software, the heat transfer efficiency of the heat exchangers is set as 80%. The dynamic parameters of temperature, pressure and mass flow for each cold energy utilization module are obtained based on the four simulation submodels in Figures 3–6. Note that the unlabeled data is the same as the previous data by default. Table 4 shows the main operating parameter data of each node under a nominal condition.

Table 5 summarizes the simulation results regarding the whole LNG cold energy recovery process. During the first and second stages, the assignments for the cold energy utilization are as follows: (1) The energy exchangers E-1 and

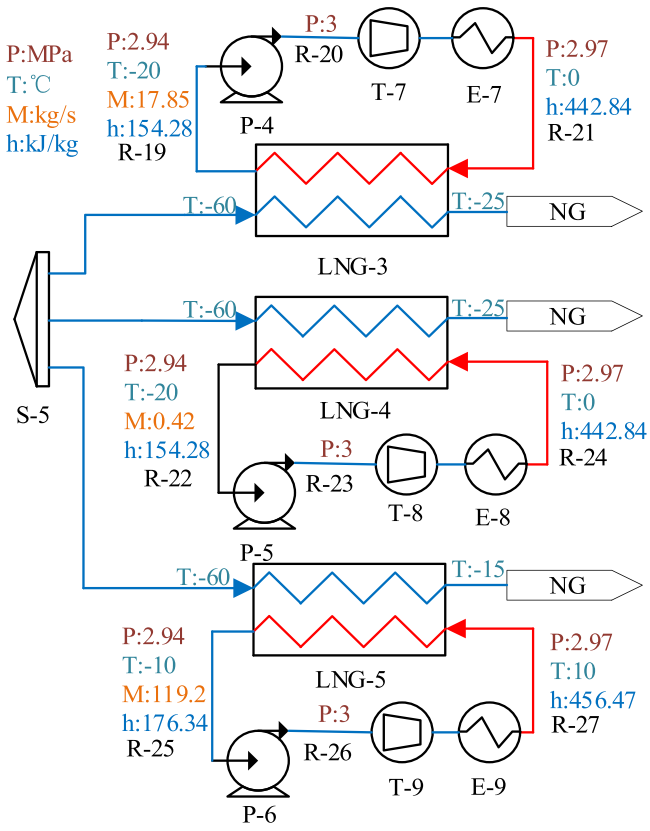


**FIGURE 6** Parameter changes during the third-stage energy exchange.

E-4 supply cold energy for the MFR; (2) The energy exchangers E-2 and E-5 supply cold energy for the APFR; (3) The energy exchangers E-3 and E-6 supply cold energy for the SR. The total cooling power for each module is 11,172, 37,810, and 1989 kW, respectively. During the third stage, the energy exchangers E-7–E-9 supply cold energy for the IMR, ISR, and AC. The total cooling power for each module is 2660, 63.3, and 20,850 kW, respectively. In sum, the total cooling power is estimated to be about 74.5 MW for the whole cold store.

For most commercial electric-driven air conditioning systems in cold stores, the coefficient of performance (COP) in cooling mode can be set as 4. Therefore, the total cooling power corresponds to 18.6 MW of electric power. This means that the annual electricity savings can be up to 162.9 GWh.

# 5 | ECONOMIC ANALYSIS AND ENVIRONMENTAL BENEFITS

## 5.1 | Investment cost estimation

The economic analysis covers the initial cost, operating cost, and profit. To better present the economic analysis

**TABLE 4** Simulation data at each node under a nominal condition.

| | *m* (kg/s) | *T* (°C) | *P* (MPa) | *h* (kJ/kg) | Fluid |
|---|---|---|---|---|---|
| L-1 | 172.45 | −162 | 0.1 | −4.04 | LNG |
| L-2 | 172.45 | −162 | 7.21 | 5.94 | LNG |
| L-3 | 172.45 | −105.5 | 7.14 | 195.82 | NG |
| L-4 | 172.45 | −60 | 7.07 | 467.54 | NG |
| L-5 | 22.3 | −60 | 7.07 | 467.54 | NG |
| L-6 | 0.53 | −60 | 7.07 | 467.54 | NG |
| L-7 | 149.62 | −60 | 7.07 | 467.54 | NG |
| L-8 | 22.3 | −25 | 7.00 | 653.83 | NG |
| L-9 | 0.53 | −25 | 7.00 | 653.83 | NG |
| L-10 | 149.62 | −15 | 7.00 | 686.14 | NG |
| R-1 | 17.74 | −55 | 0.147 | 96.79 | Ammonia |
| R-2 | 17.74 | −55 | 0.15 | 96.80 | Ammonia |
| R-3 | 3.89 | −55 | 0.15 | 96.80 | Ammonia |
| R-4 | 13.16 | −55 | 0.15 | 96.80 | Ammonia |
| R-5 | 0.69 | −55 | 0.15 | 96.80 | Ammonia |
| R-6 | 3.89 | −25 | 0.149 | 1574.1 | Ammonia |
| R-7 | 13.16 | −25 | 0.149 | 1574.1 | Ammonia |
| R-8 | 0.69 | −25 | 0.149 | 1574.1 | Ammonia |
| R-9 | 17.74 | −25 | 0.149 | 1574.1 | Ammonia |
| R-10 | 25.39 | −55 | 0.147 | 96.79 | Ammonia |
| R-11 | 25.39 | −55 | 0.15 | 96.80 | Ammonia |
| R-12 | 5.57 | −55 | 0.15 | 96.80 | Ammonia |
| R-13 | 18.83 | −55 | 0.15 | 96.80 | Ammonia |
| R-14 | 0.99 | −55 | 0.15 | 96.80 | Ammonia |
| R-15 | 5.57 | −25 | 0.149 | 1574.1 | Ammonia |
| R-16 | 18.83 | −25 | 0.149 | 1574.1 | Ammonia |
| R-17 | 0.99 | −25 | 0.149 | 1574.1 | Ammonia |
| R-18 | 25.39 | −25 | 0.149 | 1574.1 | Ammonia |
| R-19 | 17.85 | −20 | 2.94 | 154.28 | Carbon dioxide |
| R-20 | 17.85 | −20 | 3 | 154.27 | Carbon dioxide |
| R-21 | 17.85 | 0 | 2.97 | 442.84 | Carbon dioxide |
| R-22 | 0.42 | −20 | 2.94 | 154.28 | Carbon dioxide |
| R-23 | 0.42 | −20 | 3 | 154.27 | Carbon dioxide |
| R-24 | 0.42 | 0 | 2.97 | 442.84 | Carbon dioxide |
| R-25 | 119.2 | −10 | 2.94 | 176.34 | Carbon dioxide |
| R-26 | 119.2 | −10 | 3 | 176.34 | Carbon dioxide |
| R-27 | 119.2 | 10 | 2.97 | 456.47 | Carbon dioxide |

of the proposed system, some key simulation parameters are set in Table 6.

The initial investment includes land, construction, and equipment costs. The main parameters for the conventional cold store are shown in Table 7. By comparison, a conventional chiller contains a series of electric-driven compressors, but the LNG-based cold store only uses heat exchangers. So, the actual equipment cost of the designed 10 MW class cold store can be calculated as: In Table 7, the unit price of a conventional chiller subtracts the cost of compressors and adds the cost of heat exchangers.

The cost calculation of a heat exchanger device is usually based on an estimation of the heat exchange surface area $A$. A typical initial cost $C_{in}$ is as follows[37]:

$$C_{in} = 32,800\left(\frac{A}{100}\right)^{0.68}. \tag{8}$$

Since the actual cost also depends on the operating pressure and temperature, as well as the materials of construction, three factors (for cost correction) can be used for a better estimation of the capital cost $C_{ac}$:

$$C_{ac} = \delta_M \delta_P \delta_T C_{in}, \tag{9}$$

where $\delta_M$, $\delta_P$, and $\delta_T$ are the device material, pressure, and temperature dependent factors. The materials of construction use carbon steel (CS) shells and stainless steel (SS) tubes, and the maximum pressure and temperature are designed to be lower than 7 MPa and 50°C. Then the three correction factors above can be set as 1.7, 1.7, and 1, respectively.[37]

The heat exchange surface area $A$ can be calculated by[38]:

$$A = \frac{Q}{U\Delta T_m}, \tag{10}$$

where $Q$ is the heat load; $U$ is the heat transfer coefficient; $\Delta T_m$, the average temperature difference between the hot and cold sides. From an engineering perspective, the $\Delta T_m$ is almost equal to the logarithmic temperature difference $\Delta T_{LM}$:

$$\Delta T_m = \Delta T_{LM} = \frac{(T_{h,in} - T_{c,out}) - (T_{h,out} - T_{c,in})}{\ln\frac{(T_{h,in} - T_{c,out})}{(T_{h,out} - T_{c,in})}}, \tag{11}$$

where $T_{h,in}$ and $T_{h,out}$ are the inlet and outlet temperatures of the hot flow; $T_{c,in}$ and $T_{c,out}$ are the inlet and outlet temperatures of the cold flow.

TABLE 5 Simulation data of power and energy savings in the 10 MW class cold store.

| Number | Energy (kJ/day) | Power (kW) | Total (kW) | Electric power (kW) | Carbon emissions (kg) | Module |
|---|---|---|---|---|---|---|
| E-1 | $3.97 \times 10^8$ | 4593 | 11,172 | 2792.5 | 2111.1 | MFR |
| E-4 | $5.69 \times 10^8$ | 6579 | | | | |
| E-2 | $1.34 \times 10^9$ | 15,550 | 37,810 | 9452.5 | 7146.1 | APFR |
| E-5 | $1.92 \times 10^9$ | 22,260 | | | | |
| E-3 | $7.07 \times 10^7$ | 818 | 1989 | 497.3 | 376 | SR |
| E-6 | $1.01 \times 10^8$ | 1171 | | | | |
| E-7 | $2.30 \times 10^8$ | 2660 | 2660 | 665.3 | 503 | IMR |
| E-8 | $5.47 \times 10^6$ | 63.3 | 63.3 | 15.9 | 12 | ISR |
| E-9 | $1.80 \times 10^9$ | 20,850 | 20,850 | 5589.5 | 4424.2 | AC |

Abbreviations: AC, air conditioner; APFR, aquatic product freezing room; IMR, ice making room; ISR, ice storage room; LNG, liquefied natural gas; MFR, meat freezing room; storage room.

TABLE 6 Parameters for the economic analysis.

| Item | Value |
|---|---|
| Unit cost of electricity | 0.159 $/kW h[28] |
| Building discount rate | 2%[29] |
| LNG power generation | 45.24 kW h/t[30] |
| Equipment discount rate | 5%[31] |
| Equipment durability (year) | 20[32] |
| Maintenance cost | 4.75% of initial capital cost[33] |
| Carbon dioxide emissions factor | 756 g/kWh[34] |
| Number of workers | 60 |
| Water consumption | 500 t/day |

TABLE 7 Conventional cold store: initial investment.

| Module | Parameter |
|---|---|
| Land and construction | |
| Land price | 150 $/m$^2$[35] |
| Construction cost | 8 $/m$^3$[35] |
| Insulation cost | 30 $/m$^2$[35] |
| Investment in equipment | |
| Chiller | 215 $/kW[35] |
| Number of handling machinery (per unit area) | 0.12[36] |
| Investment in single handling machinery ($) | 9250[36] |

For the conventional first-stage heat exchanger, the LNG inlet temperature is −162°C, and the NG outlet temperature is set as 0°C; the seawater inlet temperature is 11.8°C, and the outlet temperature is set as 6.8°C. For a given heat load of $1.267 \times 10^8$ W, the cost of the conventional heat exchanger can be calculated by (8)–(11), which is about 3.13 M$.

In the proposed three-stage heat exchanger scheme, the two heat loads in the first and second stages are $3.28 \times 10^7$ and $4.69 \times 10^7$ W, and the three heat loads in the third stage are $4.16 \times 10^6$, $9.89 \times 10^4$, $3.26 \times 10^7$ W, respectively. For the nine different heat exchangers in Figure 2, the sum of the capital costs is about 4.42 M$.

In conventional cold stores, electric-driven compressors are usually used to convert electric energy into cold energy. Functionally, the five heat exchangers LNG1–LNG5 in Figure 2 are equivalent to the electric-driven compressors. Therefore, when a large amount of LNG cold energy is recovered through the five heat exchangers, there is no need to purchase additional compressors. This results in an obvious cost saving for developing the whole cold store.

The cost calculation of the compressor device is usually based on an estimation of the compressing power $W$.[39] shows a typical empirical cost $C_{com}$ as follows:

$$C_{com} = 7900W^{0.62}. \quad (12)$$

For the 10 MW class cold store in Table 1, there are six heat loads inside different building modules. Considering a typical COP of 4 for the cooling operating, the six compressing power ratings are estimated to be 2793, 9452.5, 497.3, 665, 15.8, and 5212.5 kW, respectively. The sum of the purchasing costs is about 5.84 M$ for the six electric-driven compressors.

In sum, according to the cold store design parameters in Section 2.1 and related cost estimating modules in Table 7, the 10 MW class cold store has the main designing results as follows: total area 50,000 $m^2$, storage volume 214,700 $m^3$, insulation area 106,900 $m^2$, refrigerating power −74.54 MW. For the proposed LNG-based system, the total investment of the cold store is 79.98 M$.

As for the operating cost of the cold store, the main parts include labor costs, water costs, refrigeration costs, equipment maintenance costs, construction and equipment depreciation costs, and so forth. For 60 workers and an annual salary of 12 k$ per worker, the annual total salary is 720 k$. For the daily ice production, the water consumption is about 500 t per day, and the resulting annual water cost is 73 k$ with a unit cost of 0.40 $/t.

Compared to the conventional cold store using electric refrigeration, LNG-based refrigeration has no electricity fee but adds additional purchasing cost for LNG cold energy. For estimating the cold energy cost, the consumed LNG in the 10 MW class cold store is assumed to be used for power generation. For a typical power generation capacity of 45.24 kWh/t, the annual LNG consumption in the 10 MW class cold store (5.44 Mt) can generate equivalent electricity of $2.46 \times 10^8$ kWh. So the purchasing cost for LNG cold energy is estimated to be 39.1 M$ with a unit cost of 0.159 $/kWh.

In addition, based on the maintenance cost rate of 4.75%, the annual equipment maintenance cost is about 3.21 M$. Based on the building discount rate of 2% and equipment discount rate of 5%, the annual depreciation costs on construction and equipment are 248 k$ and 3.38 M$, respectively. The overall annual operating cost is 48.13 M$.

## 5.2 | Profit estimation

Based on the analysis of the investment cost and operating cost, the main results of the income and expenditure of the 10 MW class cold store are listed in Table 8.

TABLE 8 Parameters for the proposed cold store income and expenditure.

| Symbol | Description | Value |
|---|---|---|
| $P_h$ | Handling fee of 1 ton in the cold store ($/t) | 4.4[36] |
| $P_s$ | Storage/frozen fee of 1 ton for products ($/d/t) | 1.5/30[36] |
| $P_c$ | Carrying fee of 1 ton in the cold store ($/t) | 2.9[36] |
| $C_c$ | Cold storage construction depreciation cost (k$/a) | 248 |
| $C_e$ | Depreciation of cold storage equipment (k$/a) | 3380 |
| $C_m$ | Equipment maintenance cost (k$/a) | 3210 |
| $C_w$ | Wages of workers (k$/a) | 120 |
| $C_{wc}$ | Water cost (k$/a) | 73 |
| $C_i$ | Incidental expense (k$/a) | 2000 |
| $C_e$ | Cold energy cost of LNG (k$/a) | 39100 |
| $C_{ii}$ | Initial investment (M$) | 79.98 |
| $C$ | Total operating cost (M$/a) | 48.13 |

The total profit of the cold store can be calculated by:

$$P = P_h + P_s + P_c - C, \tag{13}$$

where $P_h$ is the cargo handling charge, $P_s$ is the daily storage fee of the goods, $P_c$ is the charge for moving the goods, and $C$ is the total operating cost:

$$C = C_c + C_e + C_m + C_w + C_{wc} + C_i + C_e, \tag{14}$$

where $C_c$ is the depreciation cost of cold storage construction, $C_e$ is equipment depreciation cost, $C_m$ is equipment maintenance cost, $C_w$ is the cost for workers' wages, $C_{wc}$ is the water cost, $C_i$ is the cost for electricity fee and utilities, and $C_e$ is the LNG cold energy cost.

If the 10 MW class cold store operates at full capacity, the daily processing capacity is 5500 tons, the daily freezing capacity is 5500 tons, and the total storage capacity of the storage is 40,590 tons and the gross profit is about 97.1 M$/a.

The static investment payback period can be calculated by:

$$a_s = \frac{C_{ii}}{(P_h + P_s + P_c) \times \eta - C}, \tag{15}$$

where $C_{ii}$ is the initial investment, and $\eta$ is the ratio of the actual operation of the cold store over the full load.

The dynamic payback period considers the influence of time on the currency value. A discount coefficient $f$ is introduced as follows:

$$f = \frac{1}{(1+i)^n}, \tag{16}$$

where $i$ is the discount rate, with a value of 6%,[28] and $n$ is the production time and the value is 0 in the first year and increases by 1 every year thereafter. The dynamic income is:

$$P_d = f \times P. \tag{17}$$

Net present value (NPV) can be calculated by[28]:

$$\mathrm{NPV} = \sum_{j=0}^{n} \frac{P}{(1+i)^n} - C_{ii}. \tag{18}$$

Thus the dynamic payback period can be obtained when the NPV reaches 0:

$$\sum_{j=0}^{n} \frac{P}{(1+i)^n} - C_{ii} = 0. \tag{19}$$

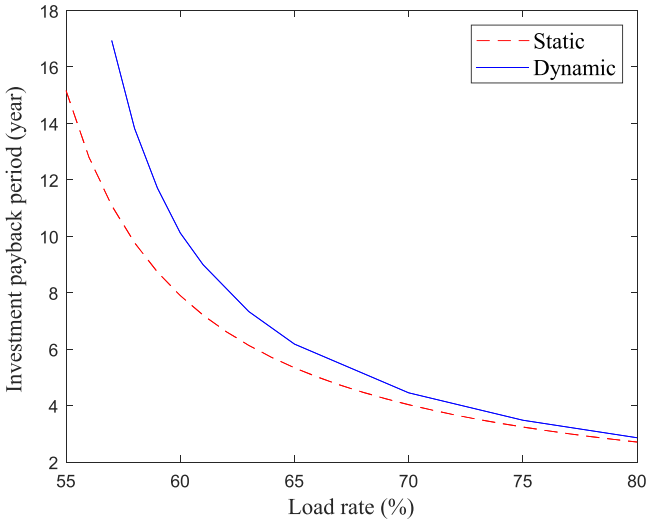


FIGURE 7 Payback periods under different operating load ratios.

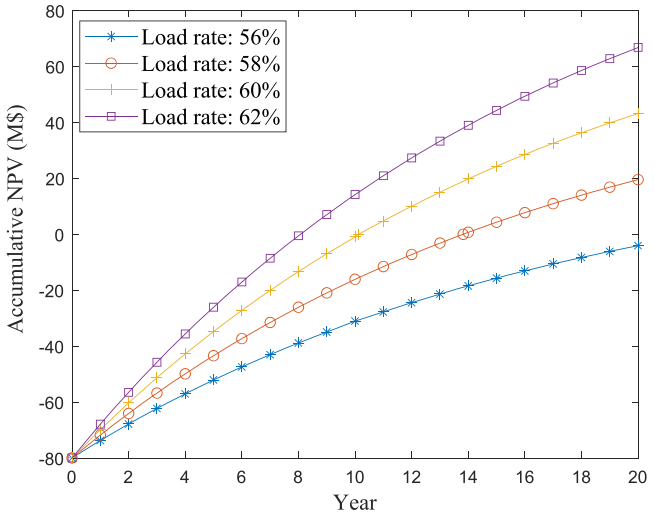


FIGURE 8 Impact of load rate of the cold store on net present value (NPV).

## 5.3 | Economic benefit analysis

The ratio of the cold storage operating load over the total load has huge impact on both the static and dynamic payback periods. As shown in Figure 7, the larger the ratio is, the lower the cold storage vacancy rate and the smaller the payback period will be. When the operating load rate of the cold store is lower than 50%, the annual income is lower than the operating cost, which means there will be no economic benefits. Due to the influence of time on currency value, the dynamic payback period is always longer than the static value. For instance, when the load rate increases to 58%, the static and dynamic payback periods are about 11.08 and 13.82 years, respectively.

Figure 8 presents the impact of the cold storage load ratio on NPV. The trend can be seen: the larger the load ratio is, with the same operating time the greater NPV, and the shorter the payback period will be. Four typical moderate-level load ratios (56%, 58%, 60%, and 62%) are given in Figure 8 The intersections of the horizontal line (NPV = 0) and each NPV curve with different load ratios represent the corresponding dynamic payback periods. When the load ratio is 56%, there is no intersection, which means the gross income over the cold store's entire life cycle (20 years) is still lower than the initial investment cost (79.98 M$), and this load ratio will not lead to any economic benefits. When the load ratio increases to 58%, 60%, and 62%, the dynamic payback periods are 13.82, 10.12, and 8.07 years, and after 20 years of the cold store's entire life cycle, the NPZs become 19.57, 43.18, and 66.79 M$, respectively. To sum up, the proposed 10 MW class LNG-based cold store has significant economic benefits from a life cycle perspective.

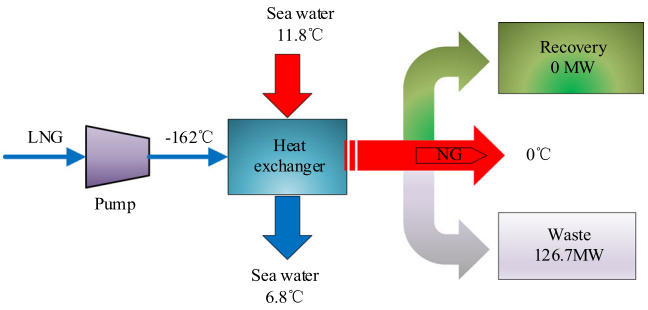


FIGURE 9 Energy flows in the conventional seawater heat-transfer scheme.

## 5.4 | Environmental benefit analysis

In general, conventional LNG gasification station uses seawater as the refrigerant. A series of single-stage heat exchangers are used to directly gasify the low-temperature LNG at −162°C, to room-temperature NG at 0°C. The conventional technology of seawater heat transfer will drain a large amount of LNG cold energy into the sea. For the LNG receiving system in this work, the LNG gasification capacity is 1.49 tons per hour. As shown in Figure 9, it will produce 126.7 MW waste of cold energy, and the annual waste of cold energy is up to 1109.9 GWh.

The multistage utilization of the LNG energy system can use a large amount of cold energy. The heat leakage in pipelines is negligible, and thus the heat exchange

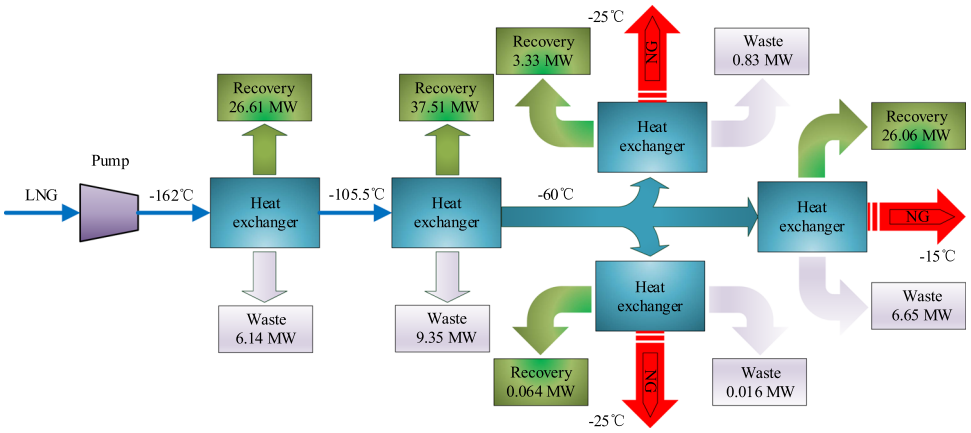


**FIGURE 10** Energy flows in the newly proposed multi-stage heat exchange scheme.

efficiency of 80% is the only major influence factor. As shown in Figure 10, the first two stages of cold energy utilization are 26.61 and 37.51 MW, respectively. The third stage of cold energy branches can use 3.33, 0.064, and 26.06 MW, respectively. This means that the gasification of the same mass of LNG can recover 93.574 MW of cold energy, and the annual recovery of cold energy is up to 819.7 GWh.

More importantly, the proposed solution of using LNG cold energy recovery avoids the utility power consumption from the fossil fuel-based main electric grid. For the 10 MW class cold store in Table 1, the annual electricity saving is about $1.63 \times 10^8$ kWh, and the saved electricity fee can be up to 16.32 M$ per year. In terms of fuel expenditure, it can save the energy of 20.05 kilotons of standard coal. Considering a typical coal power emission factor of 756 g/kWh,[34] the carbon emission reduction is up to $12.3 \times 10^8$ kg per year. From an economic perspective, this can reduce an annual carbon trading cost of 738 k$ when considering a typical carbon tax of 6 $/ton.

## 6 | CONCLUSION

In this article, a new multistage cold energy recovery/utilization scheme has been proposed for enhancing energy efficiency from the LNG receiving terminal to the coastal cold store. A realistic case in Ningbo LNG receiving station has been investigated for clarifying how to utilize the LNG cold energy in a highly efficient manner regarding the technical, economic, and environmental benefits. The main novelties, contributions, and conclusions are as follows:

(1) A new three-stage LNG cold energy recovery/utilization system has been designed by considering three cryogenic temperature ranges of −162°C to −105°C, −105°C to −60°C, −60°C to −15°C/−25°C. The dynamic energy recovery and utilization behaviors have been modeled, and the cold energy obtained has been properly assigned to different frozen areas inside a 10 MW class coastal cold store.
(2) Compared to conventional seawater heat-transfer schemes having zero cold energy recovery, the original cost for purchasing single-stage heat exchangers can be properly used to buy multistage heat exchangers in the proposed multi-stage cold energy recovery/utilization system. Moreover, about 74.86 MW of cooling power can be further used to supply the cold store when considering a typical heat exchange efficiency of 80%.
(3) Compared to conventional electric-driven cold store schemes using refrigerating compressors, the proposed solution of using LNG cold energy recovery avoids the utility power consumption from the fossil fuel-based main electric grid. For the 10 MW class cold store case study, the annual energy saving is about $1.63 \times 10^8$ kWh, and the corresponding carbon emission reduction can be up to $1.23 \times 10^8$ kg every year.

## ACKNOWLEDGMENTS

This work was supported by the Sichuan Science and Technology Program under Grant No. 2022YFG0304, and the National Training Program of Innovation and Entrepreneurship for Undergraduates under Grant No. 202110636002.

## ORCID

*Xiaoyuan Chen* http://orcid.org/0000-0002-9816-6724
*Boyang Shen* http://orcid.org/0000-0001-8169-6588

## REFERENCES


1. Safari A, Das N, Langhelle O, Roy J, Assadi M. Natural gas: a transition fuel for sustainable energy system transformation? *Energy Sci Eng*. 2019;7(4):1075-1094.
2. Howarth RW. A bridge to nowhere: methane emissions and the greenhouse gas footprint of natural gas. *Energy Sci Eng*. 2014;2(2):47-60.
3. Qyyum MA, Qadeer K, Khan MS, et al. Weed colonization-based performance improvement opportunities in dual-mixed refrigerant natural gas liquefaction process. *Energy Sci Eng*. 2021;9(2):297-312.
4. He T, Karimi IA, Ju Y. Review on the design and optimization of natural gas liquefaction processes for onshore and offshore applications. *Chem Eng Res Des*. 2018;132:89-114.
5. Khan MS, Karimi IA, Wood DA. Retrospective and future perspective of natural gas liquefaction and optimization technologies contributing to efficient LNG supply: a review. *J Nat Gas Sci Eng*. 2017;45:165-88.
6. Chen Y, Jiang S, Chen XY, Wang YF, Li T. Preliminary design and evaluation of large-diameter superconducting cable toward GW-class hybrid energy transfer of electricity, liquefied natural gas, and liquefied nitrogen. *Energy Sci Eng*. 2020;8(5):1811-1823.
7. Kumar S, Kwon H-T, Choi K-H, et al. LNG: an ecofriendly cryogenic fuel for sustainable development. *Appl Energy*. 2011;88(12):4264-4273.
8. He T, Liu Z, Ju Y, Parvez AM. A comprehensive optimization and comparison of modified single mixed refrigerant and parallel nitrogen expansion liquefaction process for small-scale mobile LNG plant. *Energy*. 2019;167:1-12.
9. Zhang F, Yu XM. LNG cold energy recovery and power generation. Paper presented at: 2009 IEEE Asia-Pacific Power and Energy Engineering Conference. 2009.
10. Kanbur BB, Xiang L, Dubey S, Choo FH, Duan F. Cold utilization systems of LNG: a review. *Renewable Sustainable Energy Rev*. 2017;79:1171-1188.
11. Mehrpooya M, Moftakhari Sharifzadeh MM, Rosen MA. Optimum design and exergy analysis of a novel cryogenic air separation process with LNG (liquefied natural gas) cold energy utilization. *Energy*. 2015;90:2047-2069.
12. Park J, Lee I, Moon I. A novel design of liquefied natural gas (LNG) regasification power plant integrated with cryogenic energy storage system. *Ind Eng Chem Res*. 2017;56(5):1288-1296.
13. Romero Gómez M, Romero Gómez J, López-González LM, LópezOchoa LM. Thermodynamic analysis of a novel power plant with LNG (liquefied natural gas) cold exergy exploitation and $CO_2$ capture. *Energy*. 2016;105:32-44.
14. He T, Nair SK, Babu P, Linga P, Karimi IA. A novel conceptual design of hydrate based desalination (HyDesal) process by utilizing LNG cold energy. *Appl Energy*. 2018;222:13-24.
15. Messineo A, Panno D. Potential applications using LNG cold energy in Sicily. *Int J Energy Res*. 2008;32(11):1058-1064.
16. He T, Chong ZR, Zheng J, Ju Y, Linga P. LNG cold energy utilization: prospects and challenges. *Energy*. 2019;170:557-568.
17. Wang X, Dennis M, Hou L. Clathrate hydrate technology for cold storage in air conditioning systems. *Renewable Sustainable Energy Rev*. 2014;36:34-51.
18. Li C, Liu J, Zheng S, Chen X, Li J, Zeng Z. Performance analysis of an improved power generation system utilizing the cold energy of LNG and solar energy. *Appl Therm Eng*. 2019;159:113937.
19. Szargut J, Szczygiel I. Utilization of the cryogenic exergy of liquid natural gas (LNG) for the production of electricity. *Energy*. 2009;34(7):827-837.
20. Peng X, She X, Li C, et al. Liquid air energy storage flexibly coupled with LNG regasification for improving air liquefaction. *Appl Energy*. 2019;250:1190-1201.
21. Mokhatab S, Economides MJ, Wood DA. Natural gas and LNG trade—a global perspective. *Hydrocarb Process*. 2006;85(7):39.
22. Ningbo Municipal Water Resources Bureau. Accessed June 29, 2022. http://slj.ningbo.gov.cn/art/2022/6/29/art_1229051365_4002777.html
23. Refrigerating Network. Accessed April 14, 2022. www.zhilengbj.cn
24. Ahmad A, Al-Dadah R, Mahmoud S. Air conditioning and power generation for residential applications using liquid nitrogen. *Appl Energy*. 2016;184:630-640.
25. Saitoh S, Daiguji H, Hihara E. Effect of tube diameter on boiling heat transfer of R-134a in horizontal small-diameter tubes. *Int J Heat Mass Transfer*. 2005;48(23-24):4973-4984.
26. Emadi MA, Pourrahmani H, Moghimi M. Performance evaluation of an integrated hydrogen production system with LNG cold energy utilization. *Int J Hydrogen Energy*. 2018;43(49):22075-22087.
27. Mosaffa AH, Mokarram NH, Farshi LG. Thermo-economic analysis of combined different ORCs geothermal power plants and LNG cold energy. *Geothermics*. 2017;65:113-125.
28. Chen X, Jiang S, Chen Y, Lei Y, Zhang D. A 10 MW class data center with ultra-dense high-efficiency energy distribution: Design and economic evaluation of superconducting DC busbar networks. *Energy Convers Manag Energy*. 2022;250:123820.
29. Demircan V, Koyuncu MA. Economic analysis of different cold storage types: a case study of Isparta province, Turkey. *Sci Pap Ser Manag Econ Eng Agric Rural Dev*. 2017;17(2):85-94.
30. Franco A, Casarosa C. Thermodynamic analysis of direct expansion configurations for electricity production by LNG cold energy recovery. *Appl Therm Eng*. 2015;78:649-657.
31. Shaibani AR, Keshtkar MM, Talebizadeh Sardari P. Thermo-economic analysis of a cold storage system in full and partial modes with two different scenarios: a case study. *J Energy Storage*. 2019;24:100783.
32. Abbasi M, Chahartaghi M, Hashemian SM. Energy, exergy, and economic evaluations of a CCHP system by using the internal combustion engines and gas turbine as prime movers. *Energy Convers Manag*. 2018;173:359-374.
33. Xu Y, Li Z, Chen H, Lv S. Assessment and optimization of solar absorption-subcooled compression hybrid cooling system for cold storage. *Appl Therm Eng*. 2020;180:115886.
34. Chen X, Chen Y, Zhang M, et al. Hospital-oriented quad-generation (HOQG)—a combined cooling, heating, power and gas (CCHPG) system. *Appl Energy*. 2021;300:117382.

35. Yan C, Shi W, Li X, Zhao Y. Optimal design and application of a compound cold storage system combining seasonal ice storage and chilled water storage. *Appl Energy*. 2016;171:1-11.
36. Ma Q, Wang W, Peng Y, Song X. A two-stage stochastic optimization model for port cold storage capacity allocation considering pelagic fishery yield uncertainties. *Eng Optimiz*. 2018;50(11):1926-1940.
37. Wildi-Tremblay P, Gosselin L. Minimizing shell-and-tube heat exchanger cost with genetic algorithms and considering maintenance. *Int J Energy Res*. 2007;31(9):867-885.
38. Hewitt GF, Pugh SJ. Approximate design and costing methods for heat exchangers. *Heat Transfer Eng*. 2007;28(2):76-86.
39. Wu S, Zhou C, Doroodchi E, Moghtaderi B. Techno-economic analysis of an integrated liquid air and thermochemical energy storage system. *Energy Convers Manag*. 2020;205:112341.

**How to cite this article:** Yue J, Feng J, Chen J, et al. Multi-stage cold energy recovery/utilization: A 10 MW class cold store with liquefied natural gas. *Energy Sci Eng*. 2022;1-14.
doi:10.1002/ese3.1373